



OPTIMUM ROTOR DESIGN OF SMALL PM BLDC MOTOR BASED ON HIGH EFFICIENCY CRITERIA

Ali Saygın¹, Cemil Ocak², Adem Dalcı³ and Emre Çelik¹

¹Department of Electrical-Electronics Engineering, Gazi University, Ankara, Turkey

²Vocational School of Technical Sciences, Gazi University, Ankara, Turkey

³Department of Electrical-Electronics Engineering, Karabük University, Karabük, Turkey

E-Mail: ademdalcali@karabuk.edu.tr

ABSTRACT

In the systems that are fed by batteries, the duration of the energy supplied to the system is of great importance. To use high efficiency-motors in these systems can extend the battery usage time and it can be said that obtaining high efficiency-motors used in low power applications is rather difficult. In this regard, in this paper, design and optimization of a brushless permanent magnet DC motor have been carried out successfully, especially for a system fed by battery. By considering the high efficiency criteria, rotor design parameters such as rotor geometry, thickness and placements of the magnets, and embrace factor have been carefully examined. By obtaining the optimal rotor geometry providing maximum motor efficiency, some informative theoretical and finite element analyses are carried out. Electrical and electromagnetic distributions gained by the changes in rotor design parameters are presented in graphics. As a result of successive steps in the paper, the efficiency is increased; the cogging torque and magnet consumption are reduced for the motor under consideration, which is 20W, 24V, 3000 rpm with an inner-type rotor.

Keywords: small PM BLDC, high efficiency, optimum rotor design.

INTRODUCTION

In recent years, high system efficiency has gained a great importance in a wide range of fields ranging from home appliances towards aviation and aerospace applications. High efficiency motors are known to play a core role in highly efficient drive systems. In traditional direct current (DC) motors, some severe problems do occur such as mechanical friction, sparks, radio interference and motor life shortening due to the brushes used for commutation. In addition to the above mentioned problems, high production costs and frequent maintenance requirements cause traditional DC motors find a limited application field nowadays. Similarly, despite simple structure, ease to be manufactured, reliable operation and low price advantages, asynchronous motors have the disadvantages of inability to start up easily and low efficiency. Moreover, speed control in a wide range in this type of motors is not economical. Other type of motor which gains popularity in recent years is the switch reluctance motor (SRM). SRMs, which are able to produce high torque at low speed, have a simple structure and low cost because of the fact that they have no windings or permanent magnets on the rotor. Nonetheless, noisy operation and fluctuations in the electromagnetic torque prevent these motors from widespread use. On the other hand, as SRMs have a low ratio value of torque/volume compared to the permanent magnet motors, they require larger geometries for the same power and torque.

For the reasons mentioned above, in small and medium scale applications, new and high performance motors are needed. Brushless DC motors (BLDCMs) in terms of being a solution to this need are used widely in battery-powered systems such as night vision cameras, hybrid vehicles, electric bicycle etc. since they have great

advantages of high efficiency, long life, low noise, ease of speed control and good torque-speed characteristics (Xia, 2012; Inoue and Nakaoka, 1998; Saygın *et al.*, 2014; Dalcı, 2014; Hanselman, 2003; Ehsani *et al.*, 2003; Ramesh *et al.*, 2011; Zheng, 2007; Nekoubin, 2011).

Torque-speed characteristic of a BLDCM is approximately a straight line drawn between the no-load speed in the vertical axis and maximum starting torque in the horizontal axis. Due to the absence of excitation losses, permanent magnet motors are more efficient than those having excitation with field windings. The importance of high efficiency for improving battery life is very clear in portable devices (Gürdal, 2015a). BLDCM output equations, such as electromagnetic torque, power and velocity are given in the relative literature (Saygın *et al.*, 2014; Hanselman, 2003; Bayındır *et al.*, 2011a; Bayındır *et al.*, 2011b; Upadhyay and Rajagopal, 2005; Koh *et al.*, 1997).

In this study, a highly efficient BLDCM has been designed for a portable system where the BLDCM is fed from battery instead of mains. In the battery-fed systems and hosting drive mechanisms, motor efficiency and size are of great importance. Therefore, in the paper, suitable motor type is determined to be BLDCM by taking previously mentioned advantages into consideration. All sizing calculations are primarily done for a 20W BLDCM. In this regard, basic design outputs such as core dimensions, slot number and dimensions, number of poles, winding type and characteristics for the corresponding motor are determined. Then, different types of rotor structures are discussed over the specified motor dimensions and the most popular five rotor types are chosen for different rotor and magnet geometries. For the selected five different rotor types, five different motors are designed without changing the stator structure,



which are given in Table 1. Of the five different motor designs performed with different rotor types, optimal rotor type is chosen according to critical parameters of efficiency, cogging torque, active material consumption (and cost). Afterwards, the study has focused on the selected optimal design and improvements are completed by performing several successive optimizations. For the selected suitable rotor type, various optimizations are carried out using the parametric approximation method for the magnet thickness and embrace values that have a large impact upon the motor performance and cost. After the successful optimization process, for the rotor type previously selected by the way of comparison, optimal magnet thickness and pole embrace values are defined. Thus, the design has been finalized by obtaining the final rotor design parameters related to the motor. For the motor under consideration, analytic analysis simulations and 2-D&3-D finite element analysis are carried out in ANSYS Rmxprt and ANSYS Maxwell, respectively. Simulation results, comparisons between the base design and optimized final design are given in detail in the forthcoming chapters.

DESIGN, ANALYSIS AND OPTIMIZATION OF MOTOR

Model of BLDCM

The power transferred to the rotor of BLDCM is obtained using equation (1).

$$P_e = e_A i_A + e_B i_B + e_C i_C \quad (1)$$

In equation (1), P_e is output power, and $e_{A,B,C}$ is the back electromotive force of the phases A, B, C, respectively. As for the input power of BLDCM, it can be calculated by equation (2).

$$P_1 = P_{cu} + P_e + P_T \quad (2)$$

In equation (3), P_T represents the switching losses, P_{cu} is stator copper losses and it is calculated by equation (3).

$$P_{cu} = r_a I^2 \quad (3)$$

Motor efficiency,

$$\eta = \frac{P_1 - (P_{cu} + P_T + P_0)}{P_1} \quad (4)$$

P_0 is the power loss at no load. Electromagnetic torque is obtained by equation (5)

$$T_e = (e_A i_A + e_B i_B + e_C i_C) / \Omega \quad (5)$$

where Ω is the mechanical speed in rad/s of the motor (Xia, 2012; Rao *et al.*, 2012).

Finite element analysis

Design of electric machines requires the solution of numerous and complex problems which are related to

the each other. Computer-aided design systems are based on the finite element method (FEM) for numerical analysis of the electromagnetic problems. FEM is a flexible and reliable method that offers short computation time and high accuracy for the calculations of magnetic fields in electrical machines (Ho and Fu, 2007; Gürdal, 2015b; Fu, 2010; Maloberti *et al.*, 2014). By means of this method, magnetic flux density (B) for each section of the machine can be calculated exactly and by exploring the probable weaknesses of the design, necessary interventions can be done (Zhou *et al.*, 2000).

The flux density distribution demonstrated in Figure 4(a) is obtained using following equations (Ho and Fu, 2007; Akbaba and Fakhro, 1992; Dalcali *et al.*, 2015):

$$\frac{\partial}{\partial x} \left(v \frac{\partial A}{\partial x} \right) + \frac{\partial}{\partial y} \left(v \frac{\partial A}{\partial y} \right) = -J \quad (6)$$

Where A is the magnetic vector potential and J is the current density which is equal to zero for steel and air parts. From equation (6), the magnetic flux density components, B_x and B_y in the x - and y -axis direction are stated as below;

$$B_x = \frac{\partial A}{\partial y} \quad (7)$$

$$B_y = \frac{\partial A}{\partial x}$$

Magnetic flux density B is calculated from equation (7).

$$B = \sqrt{B_x^2 + B_y^2} \quad (8)$$

The flux density distribution demonstrated in Figure 4(b) is obtained using following equations:

$$\frac{\partial}{\partial x} \left(v \frac{\partial A}{\partial x} \right) + \frac{\partial}{\partial y} \left(v \frac{\partial A}{\partial y} \right) + \frac{\partial}{\partial z} \left(v \frac{\partial A}{\partial z} \right) = -J \quad (9)$$

Magnetic flux density is calculated from equation (10).

$$B = \sqrt{B_x^2 + B_y^2 + B_z^2} \quad (10)$$

Selection of optimum rotor design

In the BLDCM design, five different types of rotor magnet combinations are used, which are shown in Table-1. According to the carried out analysis, some important parameters such as efficiency, cogging torque, the used amount of magnet are also presented in Table-1. In the study, the rotor-magnet combination given as Type 3 is preferred since in Type 4 and 5, the efficiency is relatively low while the cogging torque is in its highest value in Type Type 4. As for Type 2, the magnet use and the cogging torque is high, too. Because of these reasons, Types 2, 4 and 5 are eliminated. When comparing Type 1 with Type 3, by considering the cost factor, in Type 3, the use of fewer amounts of magnet and higher efficiency are



the reasons for Type 3 to be preferred among the other types. Relatively high cogging torque value is intended to be reduced with the aid of optimization process to be

performed and this reduction is the second objective of this paper.

Table-1. Five different rotor designs carried out for the selection of the optimum rotor structure.

Performance and design parameters \ Rotor types	Type 1	Type 2	Type 3	Type 4	Type 5
Efficiency [%]	83.3804	82.8079	85.1151	82.596	81.297
Cogging Torque [mNm]	19.68	34.91	23.15	38.248	10.05
Rotor-yoke flux density [T]	1.08069	1.20097	1.08522	0.658096	0.442119
Air-gap flux density [T]	0.774579	0.783716	0.7873	0.669672	0.637756
Permanent magnet weight [gr]	10.75	12.33	10.31	7.03	7.02

In Figure-1, 3D image of the initial design of a three-phase, 6-pole, 20W, 3000 rpm BLDCM with a structure of Type 3 is given beside the 1/6 part section of the full model used in the FEM, which is taken by the master-slave boundary condition.

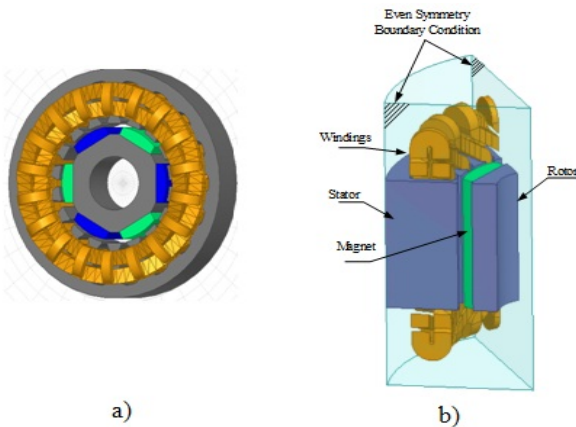


Figure-1. BLDCM a) Entire structure, b) Part section.

With respect to all parameters calculated by using analytical method, the initial design parameters of the motor are given in Table-2.

Table-2. Specification of initial design parameters.

Parameter	Value
Stator outer diameter [mm]	37.7
Length of stator [mm]	18
Stator material	M270-35A
Air gap length [mm]	0.5
Rotor outer diameter[mm]	18.2
Rotor inner diameter[mm]	9
Rotor material	ST37
Magnet Type	N40SH
Number of slots	18
Pole number	6
Rated voltage [V]	24
Rated power [W]	20

Embrace and magnet optimization

In permanent magnet machines, embrace is defined as the ratio of magnet arc to pole arc. It may also be referred to as the size of magnet surface in the radial direction and has a large influence on the cogging torque. Embrace value is also a function of magnet volume and has a great importance over the total magnet weight. Cogging torque is caused by the interaction between the magnet surface and the number of slots, and gap amount. Although it is possible to reduce cogging torque in the design phase by using combinations of distinct slot and pole numbers, in practice, making changes on the embrace value is more common to reduce cogging torque. For these reasons, in this part of the study, for cogging torque reduction, the embrace value of the structure Type 3 is optimized using the parametric approach method. Similarly, like the optimized embrace value, optimum magnet thickness is successfully determined depending upon the parametric approach.

The pole embrace and magnet thickness of a 6-pole surface magnet brushless DC motor is optimized with parametric approach via by ANSYS Maxwell package. Designers do use many methods in the design and optimization of the electrical machinery (Rong and Lowther, 1997; Nguyen and Coulomb, 1999). Parametric solution methods used in size optimization of electrical machines are widely used due to the fact that they are practical, results-oriented and fast. In the parametric solution method, solutions are performed at steps depending upon the desired accuracy by defining the lower and upper limit of the parameter to be optimized instead of assigning it a fixed value. The solution interval of the pole embrace is determined as min 0.4 and max 0.8 by taking into account the physical limitations and solution step is determined as 0.025. In the same way, the solution interval of the magnet thickness is determined as min 1mm and max 3mm by taking into account the physical limitations and solution step is determined as 0.125. The effect of the pole embrace and magnet thickness on the efficiency is given in Figure-2.

When trying to determine the optimal magnet thickness and the pole embrace, the intervals where the



efficiency is maximum and the cogging torque level is minimal should be taken into account. However, in the intervals where the efficiency is maximum, the cogging torque value may not be at low values and vice versa, in that, in the intervals where the cogging torque is minimum, the efficiency may not be maximum. Thus, individual evaluation of Figure-2 or Figure-3 will most likely lead errors. Therefore, when determining the pole thickness and embrace, they need examining together associating with one another. Also, care must be taken related to the selection of parameter values that lead to a decline in the motor power determined at the design stage.

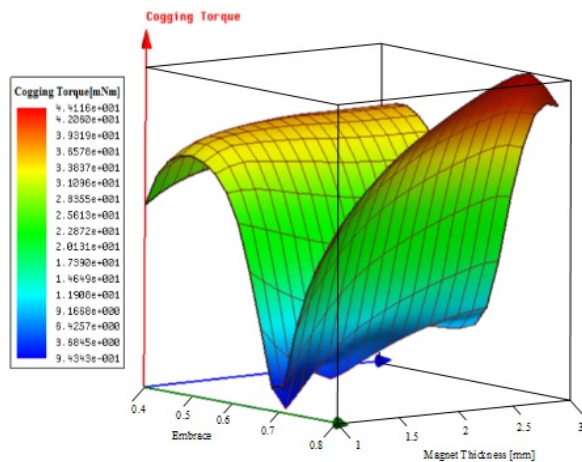


Figure-2. Efficiency against the magnet thickness and pole embrace.

In Figure 3, the change in the cogging torque is given according to the changes in the magnet thickness and pole embrace.

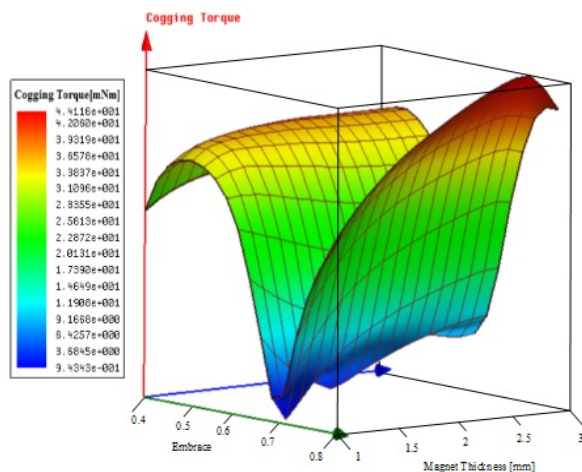


Figure-3. Cogging torque against magnet thickness and embrace.

As mentioned earlier, the cogging torque, in the permanent magnet machines, is due to the magnetic interaction between the stator and magnets placed on the rotor surface. This interaction is undesirable as it gives rise

to noise and vibration in PM motors. So, the selection of the point where the cogging torque is minimal will be correct decision. After carrying out various successive analyses, the magnet thickness and embrace value are set at 2 mm and 0.7, respectively. With the specified values, the calculated cogging torque is 9.484 mNm and the efficiency is 88.0713%.

SIMULATION RESULTS

In the transient analysis performed at the rated load, the flux density distributions obtained by the FEM in 2-D and 3-D fragmentary section are shown in Figure 4. The scale is the same for both solutions. When examining the flux density distributions, results that are consistent with the desired values are obtained. As expected, the highest value of the flux density is formed in the stator teeth and it is approximately 1,71 T. As reducing the motor size and total weight is a further aim of this study, core material that allows a flux density of about 1,8 T is chosen. Thus, the motor obtained at the end of the design is made more compact.

Figure-4. Magnetic flux density in cross sectional area a) 2D and b) 3D.

In Figure-5, the change of the air gap flux density with the magnet thickness is seen according to the electrical position of the rotor. As expected, the highest flux density is obtained as 0.791 T when using a magnet thickness of 3 mm. In the case of use of a 1mm magnet, the highest flux density is 0.658 T.

Figure-6 shows the cogging torque change with the magnet thickness according to the electrical rotor position. The cogging torque gets equal to its maximum value of 35.8 mNm when the magnet thickness is 3 mm. The design results obtained before and after the optimization process are presented in Table-3. It is apparent that the optimization has led to the increased efficiency, reduced cogging torque and magnet usage. Results also give information related to the impact of the magnet thickness and embrace values on the motor performance.

Table-3. Comparison of the analysis results of the optimized motor with the base design.

Parameter	Initial	After Optimization
Efficiency [%]	85.76	88.07
Cogging torque[mNm]	23.15	9.484
Total losses [W]	2.84	2.38
Stator-teeth flux density[T]	1.7635	1.7154
Pole Embrace	0.73	0.7
Magnet Thick. [mm]	2.2	2
Total Magnet Weight [gr]	10.31	9.2

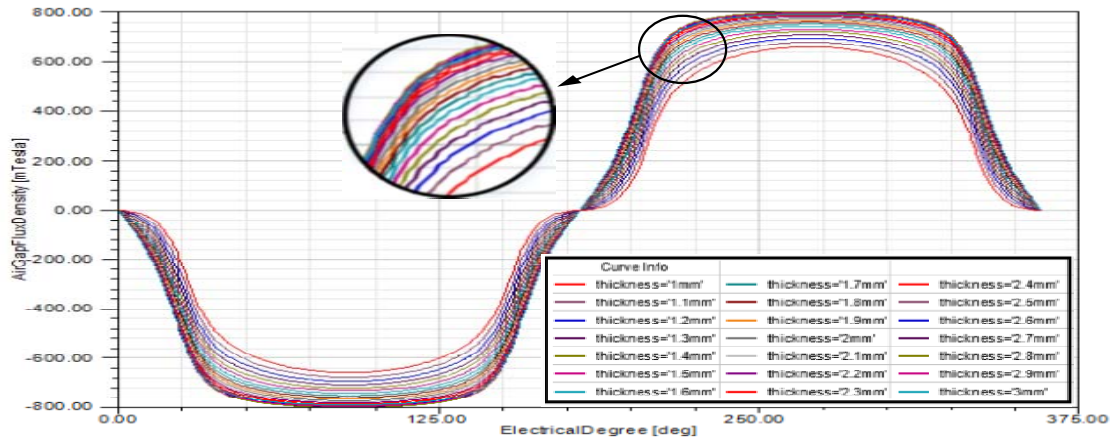


Figure-5. The change of the air gap flux density according to the electrical rotor position.

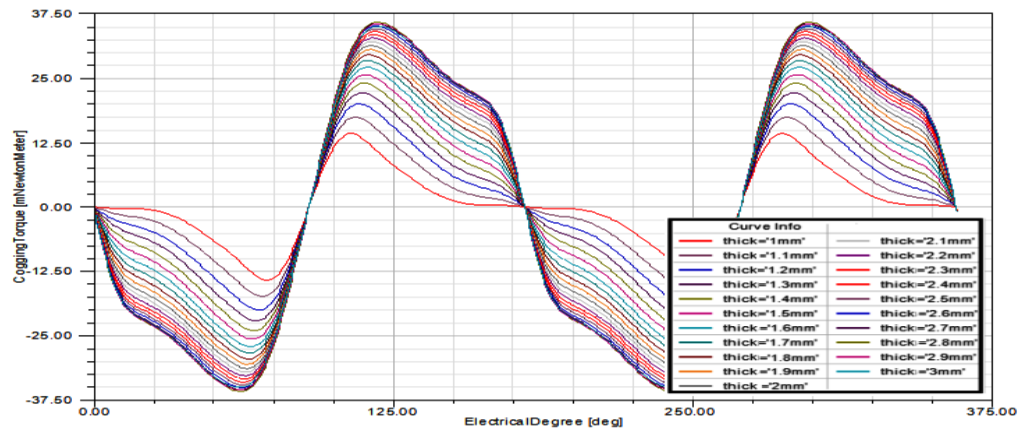


Figure-6. The cogging torque change with the magnet thickness according to the electrical rotor position.

CONCLUSIONS

In this paper, optimal rotor design for a permanent magnet brushless DC motor expected to have high efficiency and low size has been carried out, which is commonly used in battery-powered portable systems. For rotor design, five different rotor geometries and magnet structures that are commonly used in BLDCMs are taken into account. By performing various designs for each of rotor types, important performance parameters such as efficiency, cogging torque, power loss, flux density and magnet consumption are compared with one another, and on the selected structure (Type 3), embrace and magnet thickness values are optimized. At the end of the optimization process, the efficiency is increased, both the cogging torque and magnet consumption are reduced. Therefore, by investigating the effects of different rotor structures on the motor performance by means of both analytic and finite element analysis, the relationship among the desired efficiency, cogging torque and magnet consumption has been attempted to explain. The study also offers motor designers practical information that they can use in the design.

REFERENCES

- [1] Akbaba M. and Fakhro S. Q. 1992. Field Distribution and Iron Loss calculation in the reluctance Augmented Shaded Pole Motors using Finite Element Method. IEEE Transactions on Energy Conversion, Vol. 7, No. 2, pp. 302-307.
- [2] Bayındır R., Ocak C. and Topaloğlu I. 2011a. Investigation of the Effect of Magnet Thickness on Output Power and Torque of PM BLDC Machines Using Parametric Approach Method. Proceedings of the International Conference on Power Engineering, Energy and Electrical Drives, pp. 1-4.
- [3] Bayındır R., Topaloğlu I. and Ocak C. 2011b. Investigation of the Effect of Magnet Thickness on Motor Losses of PM BLDC Machines Using Parametric Approach Method. Proceedings of the International Conference on Power Engineering, Energy and Electrical Drives, pp. 1-4.



- [4] Dalcı A. 2013. Rotatif Krayojenik Soğutucular için Fırçasız Doğru Akım Motoru Tasarımı ve Optimizasyonu. Msc. Thesis, Gazi University, pp. 2-36.
- [5] Dalcı A. and Akbaba M. Comparison of 2D and 3D magnetic field analysis of single-phase shaded pole induction motors. Engineering Science and Technology, An International Journal, doi: 10.1016/j.jestech.2015.04.013, 2015.
- [6] Ehsani M., Gao Y. and Gay S. 2003. Characterization of Electric Motor Drives for Traction Application. Industrial Electronics Society, IECON'03, The 29th Annual Conference of the IEEE, pp. 891-896.
- [7] FU W. N. 2010. A Versatile Finite Element Model of Electric Machines. Electric Power Components and Systems, Vol. 31, No.10, pp. 941-966.
- [8] Gürdal O. 2015a. Design of Electrical Machines. Bursa Orhangazi University Publications, pp. 177-196 (in Turkish).
- [9] Gürdal O. 2015b. Electromagnetic Field Theory. Bursa Orhangazi University Publications, pp. 428-459 (In Turkish).
- [10] Hanselman D. 2003. Brushless Motor Fundamentals and Magnetic Modeling Brushless Permanent Magnet Motor Design 2nd Ed. Magna Physics Publishing, pp. 15-115.
- [11] HO S. L. and FU W. N. 2007. Review and Future Application of Finite Element Methods in Induction Motors. Electric Machines & Power Systems, Vol. 26, No. 2, pp. 111-125.
- [12] Inoue K. and Nakaoka M. 1998. Autotuning gain parameter implementation with fuzzy learning control scheme for DC brushless servo system. IEE Proc. Control Theory Appl., Vol. 145, No. 5, pp. 419-427.
- [13] Koh C. S., Nam W., Yoon H. S. and Choi H. S. 1997. Magnetic Pole Shape Optimization of Permanent Magnet Motor for Reduction of Cogging Torque. IEEE Transactions on Magnetics, Vol. 33, No. 2, pp. 1822-1827.
- [14] Maloberti O., Figueredo R., Marchand C., Choua Y., Condamin D., Kobylanski L. and Bomme E. 2014. 3D-2D Dynamic Magnetic Modeling of an Axial Flux PM Motor with Soft Magnetic Composites for Hybrid Electric Vehicles. IEEE Transactions on Magnetics, Vol. 50, No. 6, pp.1-10.
- [15] Nekoubin A. 2011. Design a single-phase BLDC Motor and Finite-Element Analysis of Stator Slots Structure Effects on the Efficiency. World Academy of Science, Engineering and Technology, Vol. 53, pp. 883-890.
- [16] Nguyen T. N. and Coulomb J. L. 1999. High order FE derivatives versus geometric parameters. Implantation on an existing code. IEEE Trans. Magn., Vol. 35, pp. 1502-1505.
- [17] Ramesh M. V., Amarnath J. Kamakshaiah S. and Rao G.S. 2011. Speed Control of Brushless DC Motor by Using Fuzzy Logic PI Controller. ARPN Journal of Engineering and Applied Sciences, Vol. 6, No. 9, pp. 55-62.
- [18] Rao A. P. C., Obulesh Y. P. and Babu Ch. S. 2012. Mathematical Modeling of BLDC Motor with Closed Loop Speed Control Using PID Controller Under Various Loading Conditions. ARPN Journal of Engineering and Applied Sciences, Vol. 7, No. 10, 1321-1328.
- [19] Rong R. and Lowther D. A. 1997. Applying response surface methodology in the design and optimization of electromagnetic devices. IEEE Trans. on Magn., Vol. 33, pp. 1916-1919.
- [20] Saygın A., Ocak C., Dalcı A., Gürdal O., Alantar S. and Tarhan Y. 2014. Influence of Pole Arc Offset on the Field and Output Parameters of Brushless DC Motors. International Journal of Advancements in Electronics and Electrical Engineering, Vol. 3, No. 1, pp. 47-51.
- [21] Upadhyay P. R. and Rajagopal K. R. 2005. FE Analysis and CAD of Radial-Flux Surface Mounted Permanent Magnet Brushless DC Motors. IEEE Transactions on Magnetics, Vol.41 No. 10, pp. 3952-3954.
- [22] Xia C-L. 2012. Permanent Magnet Brushless DC Motor Drives and Controls. John Wiley & Sons Singapore Pte. Ltd. Publisher, pp. 1-14.
- [23] Zheng P., Zhao J., Han J., Wang J., Yao Z. and Liu R. 2007. Optimization of the Magnetic Pole Shape of a Permanent-Magnet Synchronous Motor. IEEE Transactions on Magnetics, Vol.43, No. 6, pp. 2531-2533.
- [24] Zhou D., Rajanathan C. B., Sapeluk A. T. and Özveren, C. S. 2000. Finite-Element-Aided Design Optimization of a Shaded-Pole Induction Motor for Maximum Starting Torque. IEEE Transactions on Magnetics, Vol. 36, No. 5, pp. 3551-3554.